Determination of Liquid Water Altitudes Using Combined Remote Sensors

MARCIA K. POLITOVICH

National Center for Atmospheric Research, Boulder, Colorado

B. BOBA STANKOV AND BROOKS E. MARTNER

NOAA Environmental Technology Laboratory, Boulder, Colorado

(Manuscript received 25 August 1994, in final form 20 March 1995)

ABSTRACT

Methods by which altitude ranges of supercooled cloud liquid water in the atmosphere may be estimated are explored using measurements from a combination of ground-based remote sensors. The tests were conducted as part of the Winter Icing and Storms Project that took place in eastern Colorado during the winters of 1990, 1991, and 1993. The basic method augments microwave radiometer measurements of path-integrated liquid water with observations from additional remote sensors to establish height limits for the supercooled liquid. One variation uses a simple adiabatic parcel lifting model initiated at a cloud-base height determined from a ceilometer, temperature and pressure from a radio acoustic sounding system or rawinsonde, and combines these with the radiometer's total liquid measurement to obtain an estimate of the liquid cloud-top height. Since it does not account for liquid loss by entrainment or ice–liquid interaction processes, this method tends to underestimate the true liquid cloud top; for two cases examined in detail, 54% of icing pilot reports in the area were from above this estimated height. Some error is introduced due to differences in sampling locations and from horizontal variability in liquid water content. Vertical cloud boundaries from a K_a-band radar were also used in the study; these often indicated thicker clouds than the liquid-layer depths observed from research aircraft, possibly due to the ambiguity of the ice–liquid phase distinction.

Comparisons of liquid vertical profiles are presented, using normalized profile shapes based on uniform, adiabatic, and aircraft-derived composite assumptions. The adiabatic and climatological profile shapes generally agreed well with measurements from a research aircraft and were more realistic than the uniform profile. Suggestions for applications of these results toward a real-time aviation hazard identification system are presented.

1. Introduction

Knowledge of the location and amount of cloud liquid water in the atmosphere has useful applications in the fields of aircraft icing, numerical model initialization, and weather modification. These fields have focused much attention and research on the determination and forecasting of supercooled liquid water (SLW). In situ measurements by research aircraft have been the primary source of this kind of information. At present, no single instrument can reliably and accurately determine the location of cloud liquid water, but combinations of remote sensors might be able to achieve this goal.

Dual-channel microwave radiometers have long been used to measure integrated liquid water (ILW) in nonprecipitating clouds (Hogg et al. 1983). Many of these studies have been conducted in orographic clouds over the western United States. For example, the information provided by ground-based radiometers has been used to identify cloud seeding opportunities as described by Snider and Rottner (1982). Heggli and Rauber (1988) combined microwave radiometer measurements with soundings and aircraft sets to evaluate the climatology of cloud liquid water over the Sierra Nevada of northern California. This allowed them to determine the airflow regimes and synoptic patterns that favor formation of supercooled liquid water in orographic clouds. In this and other studies (including Rauber et al. 1986), an inverse relation between SLW aloft and precipitation at the ground was recorded. A three-year study reported by Super et al. (1986) of clouds over Grand Mesa in western Colorado also related ILW amounts to storm type. Results were similar to those from over other mountain ranges in the western United States, including the aforementioned studies of Sierra Nevada and over the Tushar Range in Utah (see Sassen et al. 1986).

Whereas cloud seeders intentionally seek SLW in order to convert it to ice crystals and improve upon natural precipitation-forming processes, pilots prefer not to encounter the aircraft icing hazard posed by encountering SLW during flight. For cloud seeding operations, the mere indication of the presence of liquid may be adequate. However, aircraft-icing applications

Corresponding author address: Dr. Marcia K. Politovich, National Center for Atmospheric Research, P.O. Box 3000, Boulder, CO 80307.

need a more precise determination of flight levels at which the SLW is expected in order to route aircraft away from these potentially hazardous areas. Used alone, microwave radiometers provide no information about the liquid's vertical distribution and cannot distinguish between supercooled and nonsupercooled liquid. However, with additional information on cloud-base and cloud-top heights and temperature profiles, the radiometer data can be extended to determine the altitude range within which the presence of supercooled liquid water is likely. Candidate sources for this additional information include ceilometers and short-wavelength radars, as well as appropriate assumptions and simple cloud models. Such a combination offers the potential for continuous, unattended, monitoring of SLW conditions aloft.

One of the first studies to use radiometers to identify in-flight icing environments was that of Popa Fotino et al. (1986), who showed that, for data collected during one winter near Denver, Colorado, the presence of ILW values at least 0.1 mm corresponded well with nearby pilot reports (PIREPs) of icing. Within 10 nautical miles (n mi), 75% of icing PIREPs were accompanied by ILW above this threshold; when the range was extended to 50 n mi, 64% were included.

As additional measurements were added to the ILW information from radiometers, more useful estimates of icing-hazard altitudes were obtained. Realizing the limitations in using radiometer data alone, Popa Fotino et al. (1989) made an initial attempt to delineate the altitude bounds of the icing hazard. The lower bound was assumed to be cloud base or the 0°C level, whichever was higher. The upper bound was either cloud top or the −20°C level, whichever was lower. Cloud base was obtained from research aircraft measurements. Cloud top was obtained from satellite infrared radiometer measurements, converted to altitude using data from a nearby, recent radiosonde or temperature measurements from the research aircraft. Two cases were presented that showed that these estimates provided reasonable, if somewhat generous, vertical boundaries for the icing-hazard layer.

Results from the Popa Fotino study were encouraging in showing that if appropriate data were available, at least a rough estimate of altitude limits for SLW could be inferred. However, the research aircraft datasets used in that study are not routinely available, and continuous monitoring by this method is therefore not feasible. More recent studies have used temperature soundings from National Weather Service (NWS) rawinsondes or RASS (radio acoustic sounding system) coupled with integrated liquid and vapor data from ground-based radiometers to develop methods by which SLW altitudes may be further determined. Case studies that make preliminary use of this information have been presented by Stankov et al. (1992), Stankov and Bedard (1994), and Politovich et al. (1992) to identify areas of aircraft icing. This paper provides a more comprehensive comparison of icing altitude estimates and an evaluation of liquid profiling methods, and represents the most complete and current research on the subject.

In this paper, measurements from a combination of remote sensors are used to obtain an estimate of the altitude range of SLW in the atmosphere. Several methods are presented and their use is illustrated using examples based on remote and in situ measurements of clouds near Denver, Colorado. The information provided through use of these techniques may be useful for real-time monitoring of aircraft icing conditions, for meteorological data assimilation schemes, or for initialization of numerical weather forecast models. A companion paper by Stankov et al. (1995) describes details of the retrieval algorithms used to derive simultaneous vapor and liquid profiles.

2. Instruments

Measurements were obtained as part of the Winter Icing and Storms Project (WISP) in northeastern Colorado. Numerous remote and in situ sensors were deployed for the study of winter storm structure and evolution (Rasmussen et al. 1992) with emphasis placed on conditions leading to aircraft icing. Data from three different field efforts were included: WISP90 (1 February–15 March 1990), WISP91 (15 January–30 March 1991), and WISPIT (WISP Instrument Test, 16 February–15 March 1993). Figure 1 shows the

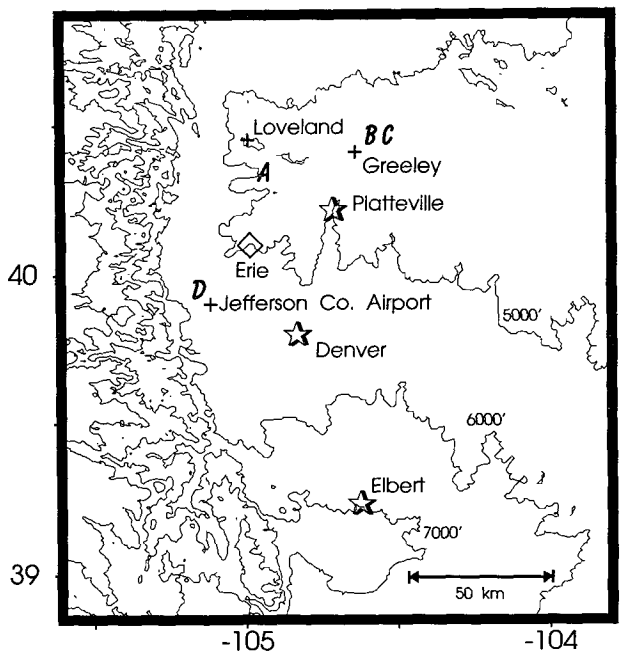

FIG. 1. The WISP area. Instrument sites and aircraft sounding locations (letters refer to cases in Table 5) are indicated. Terrain contours for 5000, 6000, and 7000 ft (1520, 1630, and 1740 m) MSL are indicated.

WISP facility locations. Table 1 lists the instruments used in this study for each year of WISP, and where they were sited.

To estimate altitudes at which supercooled liquid resides in the atmosphere, the following information is needed:

- integrated liquid water—to establish the amount of liquid (source: microwave radiometer)
- temperature sounding—to determine whether the liquid is supercooled (source: RASS, rawinsonde, or automated reports from aircraft)
- liquid cloud-base altitude—to determine the lower limit of cloud liquid (source: ceilometer or short-wavelength radar)
- liquid cloud-top altitude—to determine the upper limit of cloud liquid (source: adiabatic lifting model or short-wavelength radar).

Additionally, a description of the shape of the liquid profile may be desired to quantify the liquid amount as a function of height.

The National Oceanic and Atmospheric Administration (NOAA) Environmental Technology Laboratory (ETL) operated dual-channel (20.6 and 31.65 GHz) microwave radiometers at Platteville, Elbert, and Denver during the WISP field studies (Fig. 1). The radiometer characteristics and the retrieval technique used to determine integrated vapor and liquid values are described by Hogg et al. (1983b). Measurements were recorded every 2 min during WISP storm events and were corrected using a quality-control algorithm (Stankov et al. 1990). Spurious values were occasionally recorded during periods of light snowfall with surface temperatures near 0°C due to accumulations of melting snow on the antenae. These times were identified by the quality-control methods and resulting erroneous measurements were eliminated from the analysis. A spinning plate reflector was installed and tested on the Platteville radiometer during WISPIT (see Jacobsen and Nunnelee 1994), and was found to be generally successful in eliminating this problem. Theoretical predictions, valid for nonprecipitating clouds, indicate that the radiometer can achieve ILW measurements with about 10% accuracy (Westwater 1993). Hill (1992) presented simultaneous measurements of ILW obtained from an aircraft-based liquid probe and a ground-based radiometer that showed good agreement between the values, with a correlation coefficient of 0.94.

The National Center for Atmospheric Research (NCAR) launched Cross-chain Loran Atmospheric Sounding System (CLASS) balloon-based sondes during winter storms that provided temperature, dewpoint temperature, and wind profiles at 3-h intervals during the case studies discussed in this paper. Virtual temperature profiles with 20-min resolution were obtained from the ETL RASS at Platteville and Denver (DEN) (see May et al. 1988) for several cases presented in this paper. The RASS technique combines an acoustic source with a wind-profiling radar to detect and measure the Doppler shift of the ascending acoustic pulse. The speed of the pulse is related to the virtual temperature. The Platteville system uses a 50-MHz profiler and covers an altitude range of about 2–6 km AGL with 300-m resolution. The DEN system is at 915 MHz with a range of 0.3–2.0 km AGL and resolution of 150 m. Soundings and surface measurements were merged and interpolated to provide a continuous profile from 0.3–6 km AGL. Comparisons of RASS temperatures with those from NWS rawinsondes indicate accuracies of about ±1°C for the RASS (Martner et al. 1993b). The difference between the virtual and sensible temperature at saturation for 0°C is 0.75°C.

Cloud-base height was obtained from a lidar ceilometer operated by the Denver National Weather Service. This instrument measures the height of cloud base with 50-m resolution up to 3.7 km AGL at 0.5-min intervals (Schubert et al. 1987). During WISPIT an additional lidar ceilometer was installed at Platteville to provide ceiling height measurements at 1-min intervals. The ETL K_a-band radar (8.7-mm wavelength) was used during WISP91 and WISPIT to detect cloud layers. Its excellent sensitivity (−30 dBZ at 10-km range) and resolution (37.5-m gates) enable it to obtain detailed measurements of weak clouds. Its use in detection and tracking of clouds has been demonstrated during several recent projects (Martner and Kropfli 1993). Both the ceilometer and K_a-band radar may erroneously interpret precipitation as a cloud-base measurement. Cloud-top temperatures obtained from infrared satellite imagery displayed on an integrated weather display workstation developed by the NOAA Forecast Systems Laboratory (Bullock et al. 1988) were also used in this study.

TABLE 1. Combined remote sensor study instruments. The Wyoming aircraft is the University of Wyoming King Air; the NCAR aircraft is the NCAR King Air. Ground-based instrument locations are indicated in Fig. 1.

		Remote sensors					
Year	Aircraft	Liquid probe	Radiometer	Ceilometer	RASS	Radar	CLASS
1990	Wyoming	CSIRO	Denver	Denver	n/a	n/a	Loveland
1991	Wyoming	FSSP	Platteville	Platteville	Platteville	Erie	Loveland
1993	NCAR	CSIRO	Platteville	Platteville	Platteville	Platteville	Platteville

Airborne measurements of liquid water used for technique development and verification of the remote sensor data during WISP90 and WISP91 were provided by the University of Wyoming King Air research aircraft. Instrumentation onboard this aircraft is described fully by Cooper et al. (1984); those measurements pertinent to this study include temperature, which was measured using a reverse-flow probe (Rodi and Spyers-Duran 1972), and liquid water content. During WISP90, liquid water measurements from a CSIRO (Commonwealth Scientific and Industrial Research Organization) probe (King et al. 1978) were used; for WISP91 a Particle Measurement Systems (PMS) forward-scattering spectrometer probe (FSSP) corrected for airspeed effects (Cerni 1982) was used. During WISPIT, the NCAR King Air obtained in situ cloud measurements. An FSSP was used for liquid water content data; the measurements were corrected for true airspeed effects and for coincidence errors as per Cooper (1988). Errors in liquid water measurements from the FSSP are reported at 34% by Baumgardner (1983). King et al. (1978) claimed an accuracy in CSIRO-measured liquid water content of 8% at 0.5 g m^{-3} and 16% at 0.2 g m^{-3}. These are laboratory-condition values; in practice the liquid measurement errors may be considerably larger. The FSSPs used in the studies were calibrated prior to and after the field projects to ensure sizing was accurate, and the instrument windows were cleaned frequently during the projects. Ice crystal measurements were obtained using PMS 2D-C and 2D-P particle probes, which provide two-dimensional images of hydrometeors in the size ranges 25–800 and 200–6400 μm, respectively.

Finally, PIREPs of icing were used to verify where and when icing conditions existed in the WISP area. Since aircraft icing is defined as the accretion of SLW on the airframe, PIREPs can be used as positive indicators of SLW. However, these are not highly reliable sources of data. Their shortcomings, described by Politovich and Olson (1991), Brown et al. (1993), and others, include subjectivity, infrequent and intermittent reporting, and errors in altitude and position.

TABLE 2. Aircraft liquid-cloud data used in this study. Bases and tops are for the liquid cloud as described in the text. Level flight legs are periods in liquid cloud with gaps less than about 1 km.

Date	Number	Base (km MSL)	Top
a. Cloud soundings			
13 Feb 1990	3	1.9	3.1–3.3
27 Feb 1990	1	2.6	3.2
28 Feb 1990	1	2.9	3.1
16 Jan 1991	3	2.0	2.8
19 Jan 1991	2	3.4	3.7
2 Mar 1991	2	1.8–1.9	2.0–2.3
4 Mar 1991	1	3.9	4.5
11 Mar 1991	1	5.1	5.3
12 Mar 1991	1	4.3	4.6
15 Mar 1991	2	2.6–4.6	2.7–4.8
16 Mar 1991	5	1.6–3.6	2.0–3.7
22 Mar 1991	2	3.2	3.5
27 Mar 1991	2	2.5–2.9	5.0–5.8
24 Feb 1993	10	1.7–2.0	1.8–2.5

b. Level flight segments

Date	Number
2 Feb 1990	1
13 Feb 1990	12
27 Feb 1990	3
28 Feb 1990	7
2 Mar 1991	4
16 Jan 1991	6
19 Jan 1991	2
20 Jan 1991	10
25 Jan 1991	4
5 Mar 1991	3
11 Mar 1991	1
12 Mar 1991	5
15 Mar 1991	10
16 Mar 1991	4
22 Mar 1991	8
27 Mar 1991	13
29 Mar 1991	4
24 Feb 1993	3

TABLE 3. Aircraft liquid cloud statistics for the 36 cloud soundings listed in Table 2. Ice concentration represents total accepted images (minus streakers and other artifacts) from a 2D-C probe.

Quantity	Median	Minimum	Maximum
Base height (m MSL)	2024	1644	5149
Top height (m MSL)	2455	1774	5295
Depth (m)	422	103	2906
Base temperature (°C)	−6.6	−20.1	−2.3
Top temperature (°C)	−7.6	−22.6	−0.9
Maximum SLW (g m^{-3})	0.19	0.04	0.49
ILW (mm)	0.049	0.002	0.384
Average ice concentration (L^{-1})	1.78	0.0	46.9

3. Characteristics of WISP liquid clouds

During the three WISP field efforts, 36 soundings were obtained through liquid clouds with depths greater than 100 m and no vertical gaps larger than 100 m within the liquid layers. Table 2 lists the dates of the 36 soundings; Table 3 summarizes statistics from the aircraft measurements obtained during the soundings. For the aircraft measurements discussed in this paper, "in cloud" refers solely to the liquid cloud. The vertical extent of the physical cloud could be larger, since liquid layers were often embedded in a deeper ice cloud. The criteria used were that 1-s measurements of SLW content had to exceed 0.01 g m^{-3}, and cloud tops and bases had to have at least two consecutive 1-s liquid measurements. Ice was occasionally present in the liquid regions but in low enough concentrations that contamination of FSSP data as described by Gardiner and Hallett (1985) was not observed. The CSIRO data were

zeroed when the FSSP indicated no cloud (usually a threshold of 5 cm^{-3}) to account for baseline drift errors. The dates of the soundings are listed in Table 2. All clouds in this sample set resided at temperatures below 0°C; thus, all liquid was supercooled. Cloud tops were often characterized by strong inversions, so that the cloud-top temperature was not necessarily the coldest temperature in the cloud. The clouds were generally shallow, with a median depth of 422 m; the median base and top heights were 2024 and 2455 m MSL, respectively.

Figure 2 illustrates the variety of vertical profiles obtained from the 36 in-cloud soundings during WISP90 and WISP91. Although no single shape can adequately characterize every profile, the following generalization is useful. The profiles were divided into tenths along their depth, and the fractional contribution to the total liquid from each tenth was derived. A composite profile was constructed, which is described in Table 4 and illustrated in the lower right corner of Fig. 2. This composite profile can be used to distribute a radiometer's measured integrated liquid value through known or estimated cloud depths. Note that this does not represent a true climatology of the clouds in the project area, since only 36 measurements on 14 days are used, and that the results are biased toward clouds present on 24 February 1993, since 10 of the soundings were obtained on that day.

The horizontal distribution of cloud liquid is more difficult to evaluate. The clouds were generally widespread; occasionally, broken clouds were sampled with clear air in between. Figure 3 shows two examples that illustrate the variable nature of the horizontal distribution of liquid in WISP clouds. The liquid water as a function of distance along the flight tracks has the same average value (gaps included) in both cases (0.10 g m^{-3}), but their spatial characteristics are quite different. The first case, sampled 17 March 1991, was in fairly uniform cloud; the standard deviation was 0.041 g m^{-3}. The second case, 22 March 1991, was through broken cloud and had the same average SLW content but higher standard deviation, at 0.113 g m^{-3}. Both flight legs had average temperatures of −16.3°C. This illustrates the difficulties of comparing aircraft measurements obtained at locations away from the fixed-point remote sensors in that differing degrees of horizontal variability may be encountered in different

TABLE 4. Aircraft-derived composite cloud profile. This represents the average contribution to the total vertically integrated liquid water amount per tenth of the cloud depth. Layer 1 is the lowest, layer 10 the highest cloud layer. The term lwc/lwc_{max} is the average layer liquid water content divided by the maximum in the cloud.

Layer	Percent contribution	lwc/lwc_{max}
1	4.0	0.27
2	5.8	0.40
3	6.9	0.47
4	8.1	0.55
5	8.9	0.61
6	11	0.78
7	12	0.85
8	13	0.90
9	15	1.0
10	15	0.99

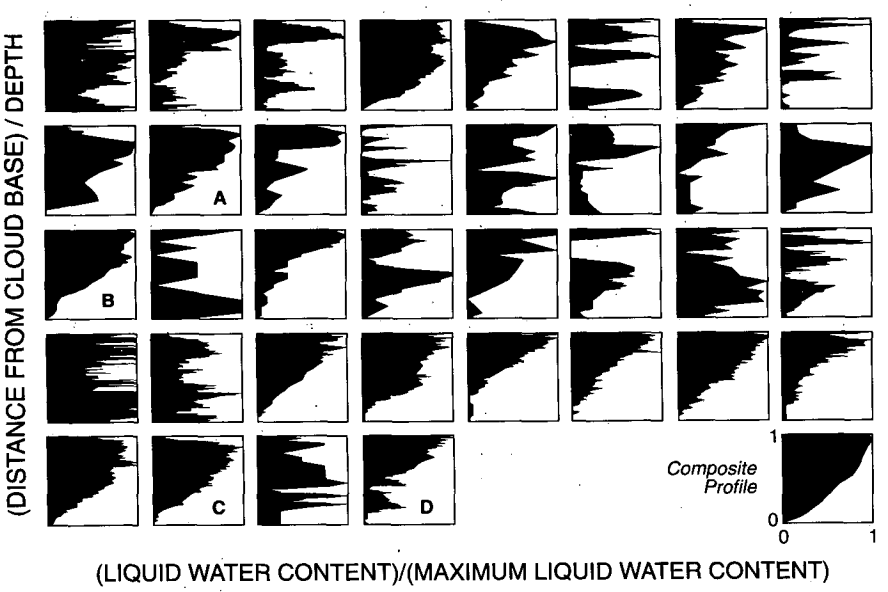

FIG. 2. Normalized vertical profiles of SLW from the WISP research aircraft. Vertical scale extends from the liquid cloud base (0) to top (1), horizontal scales are from 0 to maximum SLW content (1). The lower right-hand profile is the composite profile, as described in the text and Table 4. Lettered soundings are for cases A–D listed in Table 5.

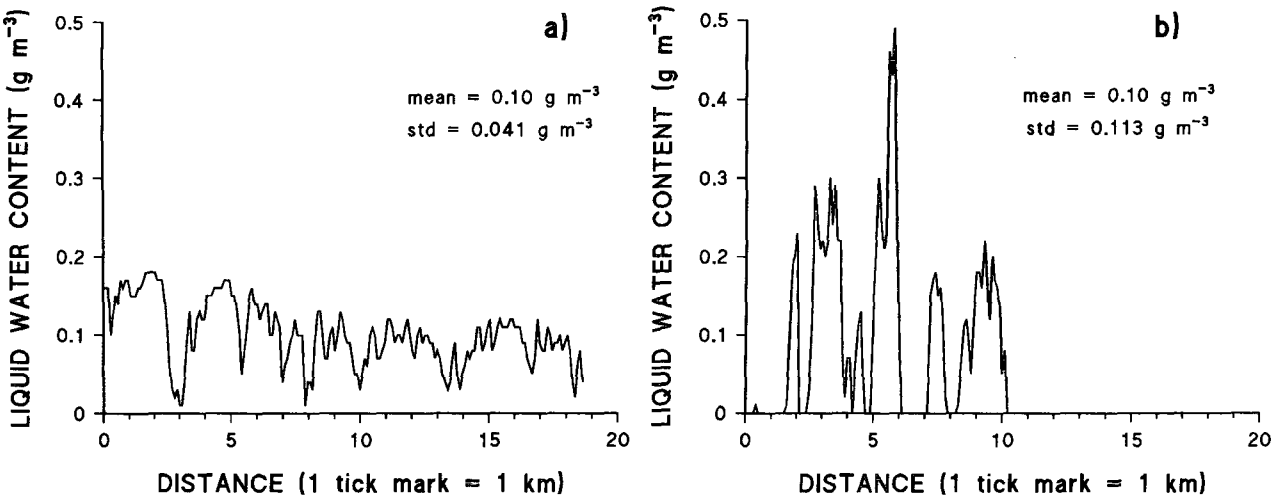

FIG. 3. SLW content plotted against distance along the flight track for two level flight periods sampled during WISP. (a) 1739:48–1743:00 UTC 17 March 1991, (b) 0858:29–0900:01 UTC 22 March 1991.

clouds. The horizontal variability of cloud liquid is a likely cause of discrepancies between the in situ and remote measurements of ILW, liquid profiles, and cloud-top and cloud-base heights.

During WISP90 and 91 and WISPIT, the Wyoming and NCAR King Airs flew 100 straight, level flight legs in cloud (Table 2). These represent a mixture of continuous and broken cloud; the aircraft changed direction or altitude for a variety of reasons so the dataset is not suitable for assessing the true horizontal extents of the clouds. Level flight segments ranged in length from 4.4 to 136.3 km, with median, 25th, and 75th percentile lengths of 19.4, 10.4, and 38.7 km, respectively. Zeroes were averaged into the datasets, but there were no gaps longer than 1 km. Liquid water contents tended to be low, with an average mean value along a level flight leg of 0.09 g m^{-3}. The average standard deviation of the liquid water content was 0.056 g m^{-3}, and the average dispersion (the standard deviation divided by the mean) was 0.92. Thus, on average, the SLW varied by ±92% of its mean value during a single cloud pass. Frequency histograms of these values are shown in Fig. 4. These statistics are presented as indications of the variability of cloud liquid at a single altitude; they are not intended to represent a comprehensive cloud climatology, which is beyond the scope of this work.

4. An adiabatic model method for estimating cloud-top altitude

In the absence of an independent remote measurement of the top of the liquid cloud, some means of its estimation is needed. If the height, temperature, and pressure at the cloud base and the total integrated liquid are known, a simple adiabatic lifting model can be applied as a lower bound to the depth of the liquid cloud (Stankov and Bedard 1994; Stankov et al. 1995). As a parcel is lifted, it cools at the moist-adiabatic lapse rate, and water is condensed. Liquid is accumulated until the value equals the ILW measured by the radiometer; this level is considered the top of the liquid layer. For a cloud base at 850 mb, 0°C, and ILW of 0.1 mm, a 2°C error in temperature results in a difference in the cloud-top height estimate of 20 m, or 7% of the adiabatic depth.

Although the adiabatic parcel lifting model is used here as a convenience, liquid-top heights estimated in this way may be subject to additional error because most WISP clouds were probably formed in a manner more accurately described as a layer lifting process. The origin of the air forming the clouds is likely tens or hundreds of kilometers upstream of the sampling location. Even those clouds that are indeed formed by lifting of parcels seldom attain fully adiabatic liquid values due to entrainment, precipitation fallout, and other factors. These important details are largely unknown for the WISP dataset, however. Furthermore, liquid is not always confined to the lowest portion of the lowest cloud layer, as this method assumes. Hence, the more tractable but less precise parcel lifting model is employed. For the 36 cloud soundings, the calculated adiabatic ILW varied from 2% to 110% of the value measured from the aircraft (see Fig. 5). The actual cloud depth ranged from 0.71 to 6.25 times the adiabatic depth. This is shown in Fig. 5b as the parameter "depth factor," which is the multiplicative factor, applied to the adiabatic model cloud depth, needed to achieve the actual cloud depth. Figure 5c shows these two parameters plotted against each other. Excluding one obvious outlier point (2%, 1.45), the equation $y = 10.3x^{-0.51}$ describes the relation between cloud depth factor y and adiabatic ILW x with a correlation coefficient of 0.995. The percentage of adiabatic ILW was

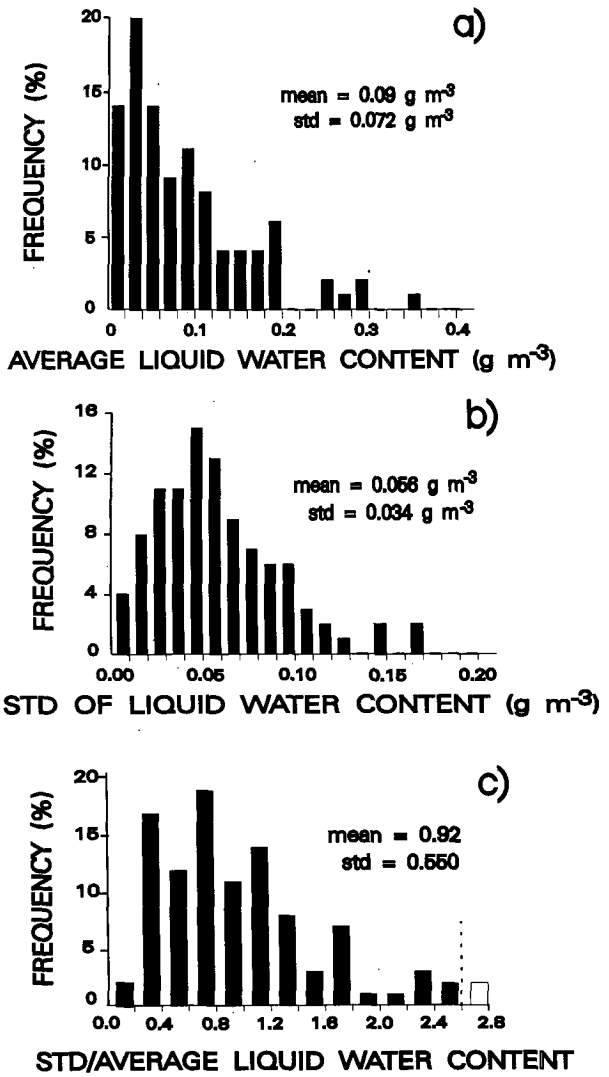

FIG. 4. Frequency histograms of (a) average, (b) standard deviation, and (c) dispersion (standard deviation divided by the average SLW content) from 100 level flight legs sampled during WISP90 and WISP91. Dates of the flight legs are listed in Table 2.

poorly related to the ice crystal concentration in these clouds; thus, factors in addition to glaciation are responsible for subadiabatic SLW contents.

The following sections discuss two WISP90 cases for which measurements were available to apply the adiabatic model cloud-top estimation method. The cases are similar, consisting of upslope (easterly flow) cloud with overlying westerly flow. Clouds were shallow with temperatures generally between 0° and −15°C, and the tops in these two cases were marked by temperature inversions. The clouds produced light snow and occasional freezing drizzle.

a. 27 February–1 March 1990

A shallow cold front moved into the Denver area from the north at about 0000 UTC 27 February. Following frontal passage, surface winds in the Front Range area turned to the southeast. The atmosphere was fairly stable, which contributed to the formation of a Denver cyclone (see Szoke 1989), a mesoscale circulation that can form downwind of the higher terrain of the Palmer Lake Divide (between Denver and Colorado Springs) under stable conditions. The circulation was capped by a nearly saturated layer leftover from the original cold front. The top of the saturated layer was marked by a strong inversion of nearly 5°C, with westerly winds aloft. Bernstein and Politovich (1993) provide additional information on this storm during which one fatal airplane accident occurred, possibly due to icing.

In addition to the Denver radiometer's ILW measurements, Fig. 6 shows a time–height display of temperature from the Loveland CLASS, cloud base from the Denver ceilometer, cloud top from the adiabatic method, pilot reports of icing, and research aircraft measurements of cloud top and base. The CLASS measurements were used in this and the following cross section since the RASS is not always capable of detecting temperature inversions such as those that existed near cloud top in these two cases. A secondary cold surge came through the WISP area from the north between 2200 and 2300 UTC 27 February. This lifted the Denver cyclone layer to form scattered clouds, while the capping moist layer above it formed a solid stratiform cloud with base and top temperatures of −7.6° and −10.3°C, respectively, as measured from the Wyoming King Air. This cloud remained in the area for almost 38 h, until 1200 UTC 1 March. ILW at Denver exceeded 1 mm, with peaks near 0.6 mm at both Platteville and Elbert. Light to moderate snow, snow pellets, and freezing drizzle were reported at the Denver NWS during a portion of the event (see Fig. 6). The fatal aircraft accident, which occurred while the airplane (a Cessna 208) descended toward Stapleton International Airport from the south, occurred at 0255 UTC 28 February, when ILW was still high.

Icing PIREPs were scattered throughout the time period, with a characteristic gap between 0300 and 1200 UTC when air traffic was low (as described by Schultz and Politovich 1992). These reports are provided at approximately 500-ft (160 m) resolution; there is some uncertainty in altitude due to possible differences between the altitude reported at the time of the report and the actual altitude at which icing was encountered. Similar uncertainty exists in horizontal position; these represent PIREPs within 100 km of Stapleton International Airport, where the radiometer was located.

The isotherms shown in Fig. 6 show a temperature inversion near the top of the cloud during most of the event. Cloud-top heights recorded during the research aircraft flight, from 2300 to 0010 UTC 27–28 February, ranged from 3.2 to 3.5 km MSL and resided within the inversion layer. Thus, the rawinsonde measurements of the height of the top of the temperature in-

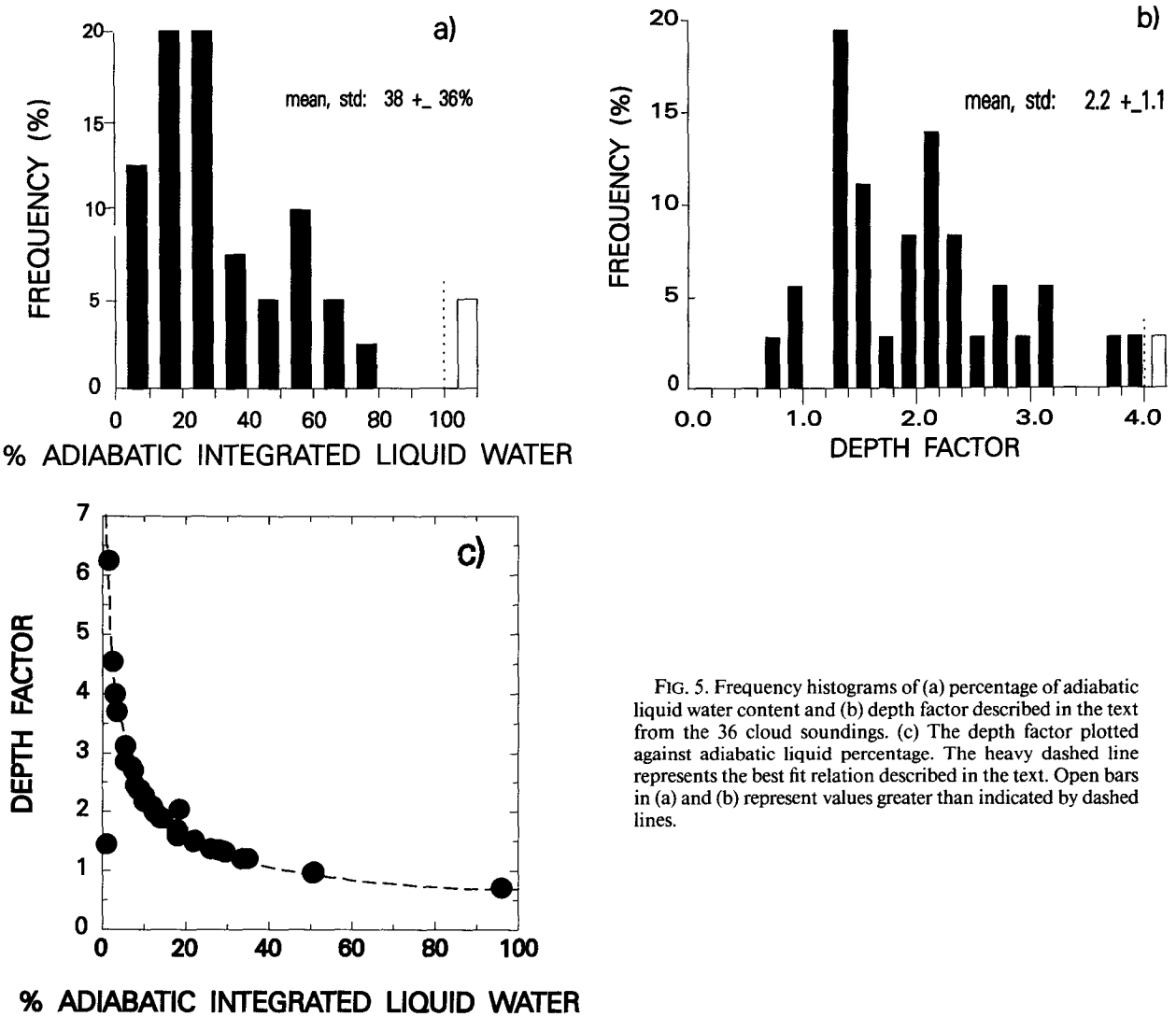

FIG. 5. Frequency histograms of (a) percentage of adiabatic liquid water content and (b) depth factor described in the text from the 36 cloud soundings. (c) The depth factor plotted against adiabatic liquid percentage. The heavy dashed line represents the best fit relation described in the text. Open bars in (a) and (b) represent values greater than indicated by dashed lines.

version may be used as an upper-bound estimate of the cloud-top height, which is also shown on the diagram. During the initial hours of cloud formation after the secondary cold surge arrived (2330–0300), the aircraft-measured, adiabatic model and inversion cloud tops are in close agreement. At approximately 0300, the cloud base lowered by about 0.7 km, as cloud formed within the cold postfrontal air rather than in the air displaced by the cold surge passage. The adiabatic model cloud top also lowered during this period, but the inversion top remained high. Unfortunately there were no research aircraft measurements nor PIREPs of cloud top available for this time period to resolve this discrepancy. Precipitation was recorded at the Denver NWS during this time, which could have reduced the cloud liquid to subadiabatic values. Later, near 0000 UTC 1 March, the two cloud-top estimates resumed closer agreement during a subsequent rise in cloud-base altitude and end of precipitation.

Figure 6b shows that many icing PIREPs originated from altitudes above the adiabatic model cloud top. Horizontal variability and subadiabatic liquid water contents may account for these discrepancies. More PIREPs are within the boundary represented by the top of the temperature inversion; however, this probably also includes a substantial volume of airspace where no cloud was present and thus would provide an overwarning of the icing hazard. Some of the higher icing PIREPs could have come from an upper-level cloud overlying the lower upslope deck, which was visible from satellite imagery and from the Wyoming King Air. Again, the adiabatic method is applied to the lowest cloud layer detected with the ceilometer, and does not account for possible liquid in additional layers.

b. 12–15 February 1990

During this storm, the radiometers detected liquid above all three sites almost continuously for over

30 h. An initial cold front passed through Denver at around 0100 UTC 13 February, as evidenced by a rapid drop in temperature near the surface (Denver's elevation is 1.6 km MSL). Scattered clouds with bases at approximately 2.4 km were present at that time, but no icing PIREPs were recorded. A more solid upslope cloud formed about 7 h later, at 0900 UTC 13 February. Data collected on two flights during this storm revealed a complex structure of liquid in two distinct layers embedded within cloud otherwise consisting

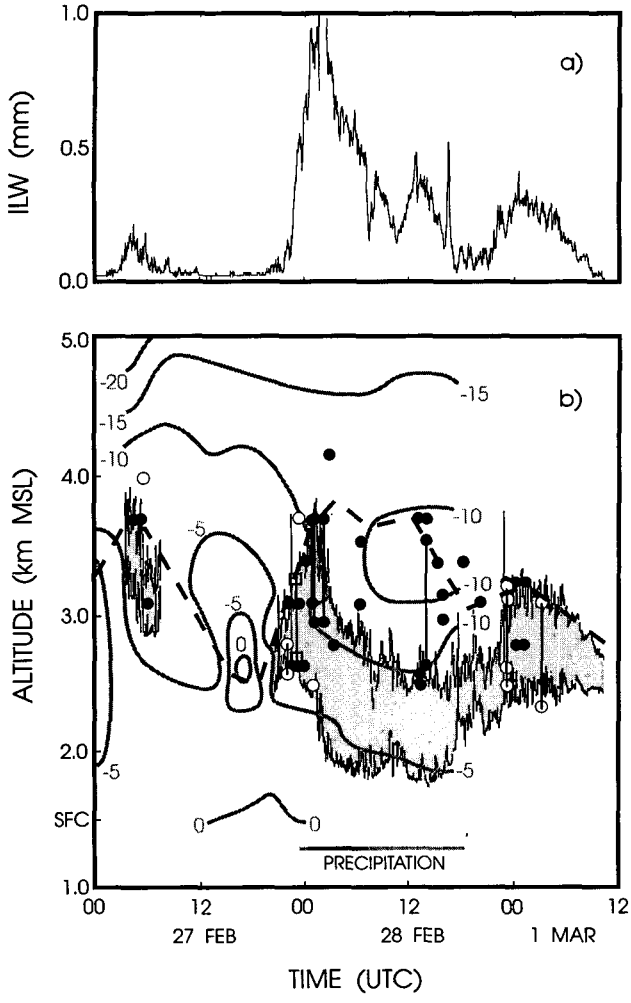

FIG. 6. Remote sensor and in situ data obtained 26 February–1 March 1990. (a) Time series of ILW from DEN radiometer. (b) Time–height cross section of several parameters including adiabatic model estimate of liquid cloud altitude (shaded) using ceilometer-measured cloud based and adiabatic model cloud top. Temperature contours (°C) from Loveland CLASS are light solid lines, dots are icing PIREPs within 50 n mi of Denver (open: severity less than moderate, closed: severity of moderate and greater), open squares are cloud tops and bases from the research aircraft. Lines join dots or squares covering a range of altitudes. The dashed line is the top of the inversion as measured by the Loveland CLASS and the Denver NWS radiosondes. The line at the bottom of the plot denotes time of precipitation at Denver NWS: light indicates light to moderate snow, dark is snow grains, ice pellets, and/or freezing drizzle.

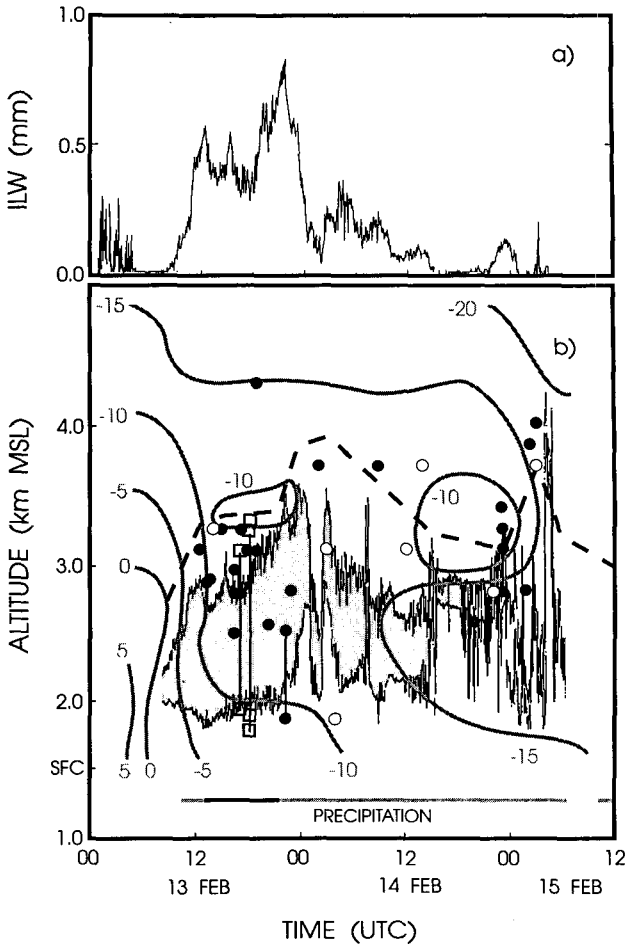

FIG. 7. As in Fig. 5 except for 12–15 February 1990.

primarily of ice crystals (Rasmussen et al. 1995). Three soundings through cloud were obtained at Jefferson County Airport, Greeley Airport, and Platteville (altitudes of the liquid cloud boundaries are shown in Fig. 7). In the lower layer, from about 1.7 to 2.5 km, liquid peaked at 0.15 g m^{-3} and was formed by upslope (easterly) flow. Above that, from 2.3 to 3.3 km,[1] liquid was produced in upward-tilted southeasterly flow that overran the lower layer; maximum values reached nearly 0.2 g m^{-3}. At the top of the upper layer, drizzle-sized droplets were observed in a stable shear region that is consistent with conditions favoring large droplet formation described by Pobanz et al. (1994). Precipitation in the form of light to moderate snow, snow grains, and freezing drizzle was recorded at the Denver NWS from 1025 UTC 13 February, through 0635 UTC 15 February.

Figure 7 shows the temperature structure, adiabatic model cloud, and PIREPs from this case. As with the

[1] There is some overlap in these altitudes due to horizontal variations in layer height.

previous case, a temperature inversion was present near the cloud top, and this may be used as an upper bound to the cloud depth. The liquid cloud-top altitudes recorded from the Wyoming King Air lay between those from the adiabatic method and the top of the temperature inversion. Most of the icing PIREPs occurred around the time of the maximum ILW, and nearly all of these were of moderate or greater intensity. However, this was also during midday when air traffic is at its busiest. As in Fig. 6, many icing PIREPs lie above the adiabatic method cloud top, but are within the upper-bound estimate provided by the temperature inversion top. The rise of this inversion top followed the rise of the adiabatic cloud top during the first few hours of cloud formation, but resided several hundred meters above it for most of the event.

c. *Summary*

For the two cases combined, 46% of the icing PIREPs were within the cloud boundaries estimated by the adiabatic model. If the estimated cloud top is extended above the adiabatic top, more reports are included. Figure 8 shows the percentage of PIREPs for the two cases that would be enclosed by the estimated cloud boundaries as a function of the cloud depth factor. For example, if the depth of the adiabatic model cloud were doubled (the median from the 36 soundings, equivalent to a depth factor of 2.0), 78% of PIREPs would be enclosed. The 25th and 75th percentile depth factor values (1.4 and 2.6) enclose 64% and 88% of the icing PIREPs, respectively. Thus, it appears the adiabatic method generally underestimates the true top of the liquid, as is consistent for subadiabatic clouds. However, if an empirical "buffer" were incorporated, the icing altitude diagnosis could be improved. The data from these two cases suggest that precipitation was at least partly responsible for the subadiabatic liquid contents.

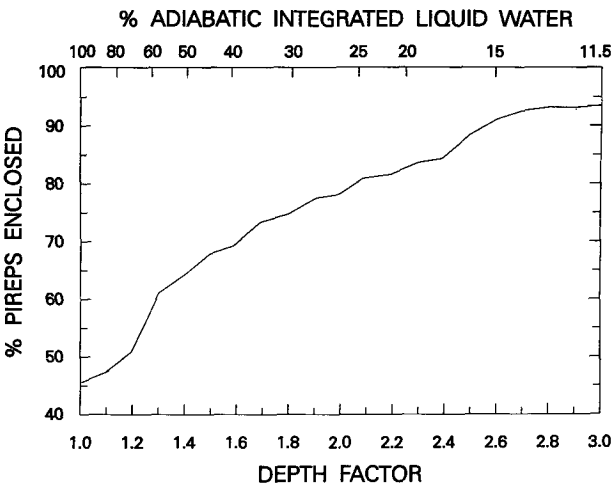

FIG. 8. Percentage of PIREPs enclosed by the cloud-top estimate as a function of depth factor applied to the adiabatic value. Data are from the two cases shown in Figs. 6 and 7.

5. Use of a K_a-band radar for cloud detection

If there are more accurate means by which cloud-top height can be obtained, the adiabatic assumption is unnecessary. For example, satellite data may be used to obtain cloud-top temperature. However, this method has several drawbacks, including obscuration or contamination of the liquid layers by overlying cirrus and matching the cloud-top temperature to the appropriate equivalent cloud-top altitude, usually done by using NWS sounding data, which have limited temporal and spatial representation. Pilot reports of the cloud-top height could also be incorporated, but these are far too intermittent and scattered.

The NOAA ETL K_a-band radar has a demonstrated capability for providing detailed depictions of cloud structure and kinematics (Martner and Kropfli 1993). The reflectivity data alone, however, are not sufficient for distinguishing liquid cloud regions from ice or mixed-phase regions. Thus, although the radar provides accurate cloud boundary information, it does not unambiguously establish the desired heights and thicknesses of liquid regions within clouds. Polarization (Matrosov and Kropfli 1993) and dual-wavelength radar techniques (Martner et al. 1993a) may be useful for distinguishing between ice and liquid, but these methods are not employed here because they are in early stages of development. Nevertheless, the radar's high-resolution reflectivity cloud echo patterns alone may be quite valuable for directing aircraft to cloud-free altitudes where icing hazards are nonexistent.

Figure 9 shows an example of complex multilayered cloud structure that this radar is capable of revealing. It shows radar reflectivity factor for a range–height indicator scan obtained at 1629 UTC 16 March 1991. This shows a thin stratus cloud, with base nearly at the ground, a middle cloud layer, which extended only 10 km horizontally, and a thicker upper-level cloud. The reflectivities are all very weak; the maximum value is -13 dBZ. The radar delineates cloud boundaries in great detail (37.5-m range resolution), but distinguishing between liquid water and ice requires more than the simple reflectivity measurements shown here.

The longer-term cloud evolution during this storm is presented in Fig. 10, which shows data from numerous sources collected 16 March 1991. The situation was shallow upslope stratiform cloud, topped by one or two additional cloudy layers. Precipitation was light snow or drizzle, when present at all; surface temperatures were around 0°C. There were few PIREPs during the time period; the lower cloud layer was quite thin (thicknesses of 103–294 m were measured by Wyoming King Air) and SLW contents were low (maxima of 0.05–0.25 g m^{-3}), thus the cloud probably did not represent an icing hazard.

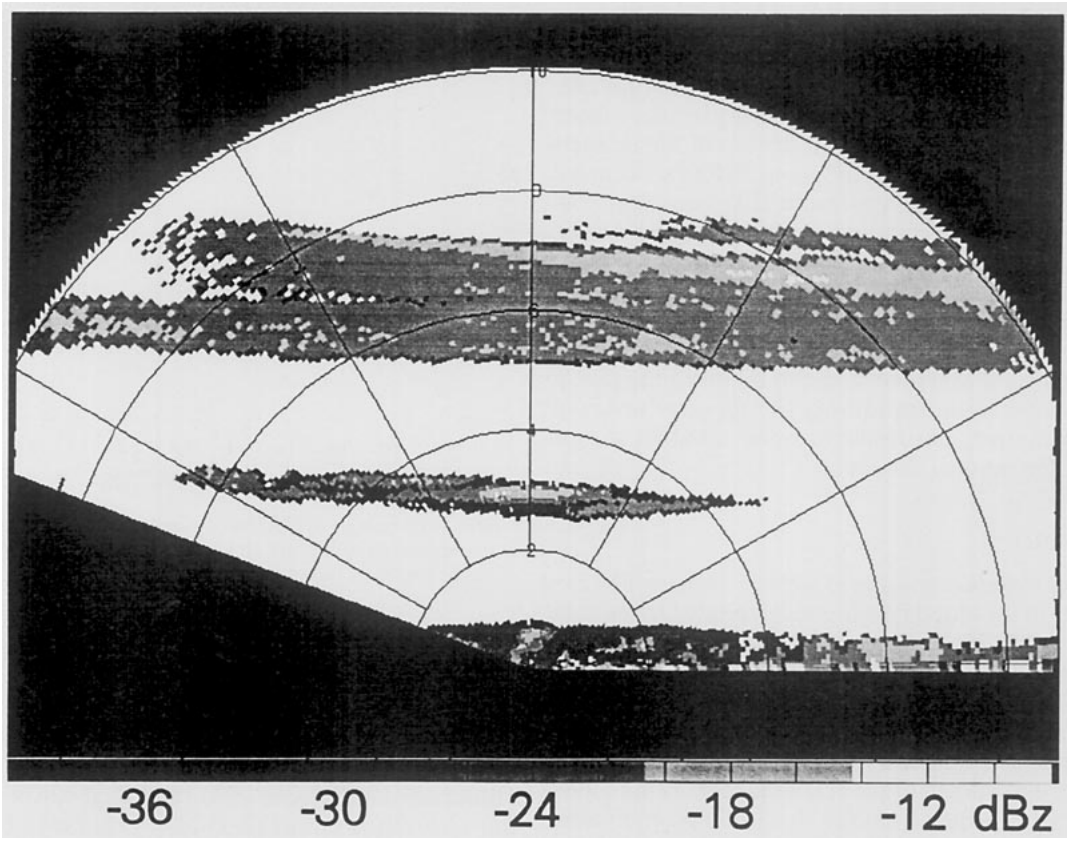

FIG. 9. Range–height indicator plot of reflectivity from the K_a-band radar. Data were obtained 1629 UTC 16 March 1991 at Erie. Orientation of the diagram is along 142°–322° radial. The dBZ values are as indicated at the gray scale at the bottom; range rings are shown at intervals of 2 km.

Cloud base from the ceilometer at Platteville, adiabatic model top from ILW measurements at Platteville, and K_a-band radar-detected cloud altitudes from Erie are shown in the figure. The aircraft sampling was restricted to the lowest cloud layer; cloud depth from the aircraft is in fair agreement with the adiabatic model, as are the radar measurements. The radar was also able to detect a fairly thick upper-cloud layer. This cloud had temperatures generally well below −15°C, and thus was likely to have been composed primarily of ice crystals rather than of water droplets. Satellite cloud tops from infrared imagery were analyzed for this case and also appear in the figure. Between 1530 and 1900 UTC 16 March, no cloud was detected from the infrared satellite imagery even though the ceilometer and radar detected clouds. Thus, the clouds must have been optically thin with significant contamination of the satellite's signal from the ground temperature.

6. Vertical profiles of liquid water

Clouds are formed in many ways under differing circumstances. Thus, there is no a priori reason to assume that an arbitrary cloud should conform to a specific liquid water profile. Nevertheless, many of the WISP aircraft soundings display common characteristics that suggest a general profile shape may often provide usefully accurate estimates for individual clouds. In this section we show results for three such cloud water profile shape assumptions to illustrate how they may be used to quantify the liquid distribution within cloud layers. Note that in any of these estimations of a vertical liquid profile, radiometer brightness temperatures were not recalculated. An iterative technique to match recorded brightness temperatures with vertical liquid distribution assumptions was done by Stankov et al. (1995); they found that the shape of the assumed profile had minimal effect on the recalculated brightness temperature.

The simplest assumption is that liquid water is distributed uniformly through the vertical extent of the cloud layer. From the vertical distributions shown in Fig. 2, this is a poor assumption but it serves as a useful first guess for radiometric inversion processes (Stankov et al. 1995) as well as for simple cloud estimates. The same adiabatic model described in the previous section for estimating the cloud-top height can also be used to provide a profile of liquid within the layer. As air parcels rise and liquid condenses, liquid increases with height in a prescribed manner assuming no depletion by en-

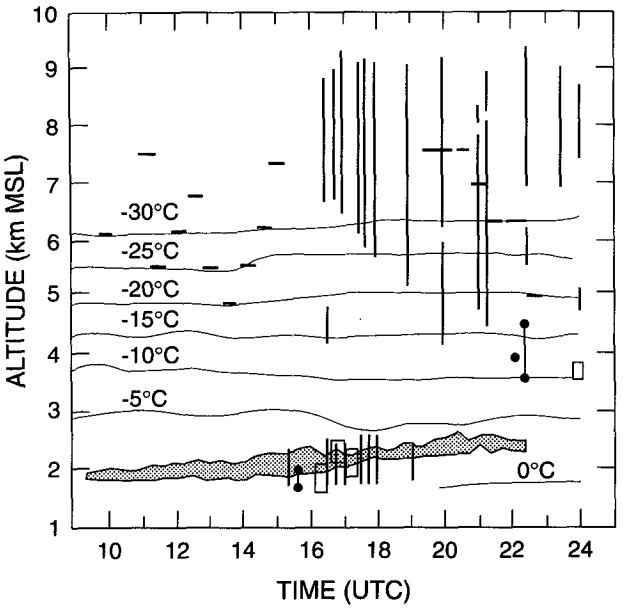

FIG. 10. Time–height cross section of data obtained 16 March 1991. Lines and symbols are the same as in Fig. 6 with the addition of horizontal bars for satellite-derived cloud tops and vertical solid lines for K_a-band cloud layers. Adiabatic model cloud calculations are every 20 min. No K_a-band measurements were made before 1500 UTC.

trainment, precipitation, or ice processes. The actual amount of liquid condensed depends upon the temperature, and to a secondary extent, on the pressure at cloud base, but the shape of the profile is similar for most temperatures. Layers (rather than parcels) of air may also be lifted to cool and form clouds; the resulting liquid profiles depend on the initial temperature and moisture profiles of the lifted air. This information, however, is not available for the WISP clouds in the dataset and is generally not available in real time for a thorough analysis of current cloud profiles. In addition, along with the lifting process, entrainment or interaction with the ice phase (e.g., preferred deposition or riming) may alter the liquid profile from an adiabatic one. Thus, an adiabatic profile may be considered an upper bound for liquid as a function of altitude. If a sufficiently large sample of in situ liquid profile measurements is available for a geographical region and cloud type, these data may be used to construct a normalized composite or climatological mean profile. Although a larger sample is desirable, such a profile was derived for the WISP aircraft dataset, as described in section 3 and summarized in Table 4. After obtaining cloud base and top and measuring the ILW, the normalized composite profile may be applied to provide an estimate of liquid water as a function of height.

Comparisons between these three profile-estimation methods and measurements obtained from research aircraft are shown in Fig. 11. The uniform, adiabatic, and composite methods were applied to soundings obtained from four flights on three days to examine their general applicability. Locations of the aircraft soundings are shown in Fig. 1 and further information on these comparisons is included in Table 5. The radar cloud bases and depths listed in this table were determined from the radar's minimum detectable signal, which is approximately -30 dBZ at a range of 10 km. The adiabatic profiles were constructed from the ceilometer measurements of cloud-base height combined with RASS temperature at cloud base and radiometer-sensed ILW. Each panel of Fig. 11 shows the actual liquid profile measured by aircraft (shaded) and the profiles estimated by remote sensors. The adiabatic profile method shape (top row) is applied between the cloud-base height measured by ceilometer and the top estimated by adiabatic lifting (cb/at, dashed lines). These bases and tops are also used for the uniform (middle) row and composite (bottom row) profile shapes. Cloud-base and cloud-top heights measured with the K_a-band radar (kb/kt, solid lines) are also shown for application of the uniform and composite shapes, but not for the adiabatic method. Temperature profiles were not available at the Erie radar site, and cloud top was directly measured with the radar.

For case A, the adiabatic model cloud depth is in good agreement with the aircraft measurements since the ILW values and cloud-base heights and temperatures matched well, and these measurements of ILW were close to the adiabatic value. The adiabatic and composite profiles applied to the adiabatic method are fairly good representations of the actual liquid profile. The K_a-band radar base is much lower than the aircraft measurement, which may be due to light precipitation. The top, however, is in good agreement, but the much larger radar depth distorts the composite profile and produces lower liquid amounts throughout the cloud than those measured in situ. The uniform profile is a poor estimate although it fares better in this case if the adiabatic method cloud boundaries are used rather than the radar boundaries.

In case B, the ceilometer- and radar-measured cloud-base heights are close to the aircraft value. However, the radiometer ILW is over twice that of the aircraft measurement and thus produces considerably higher SLW throughout the cloud for the adiabatic method applications of all three profile shape estimates. The K_a-band radar sensed cloud well above the aircraft-measured liquid cloud, which is probably due to the radar's detection of ice crystals in addition to liquid at the higher altitudes. This distributes the ILW through a larger depth and results in relatively low SLW contents.

For case C, the ceilometer measurement of cloud base is 180 m higher than that of the aircraft. However, the radiometer measurement of ILW was less than half that measured from the aircraft, which results in thin cloud-depth estimates using the adiabatic method, al-

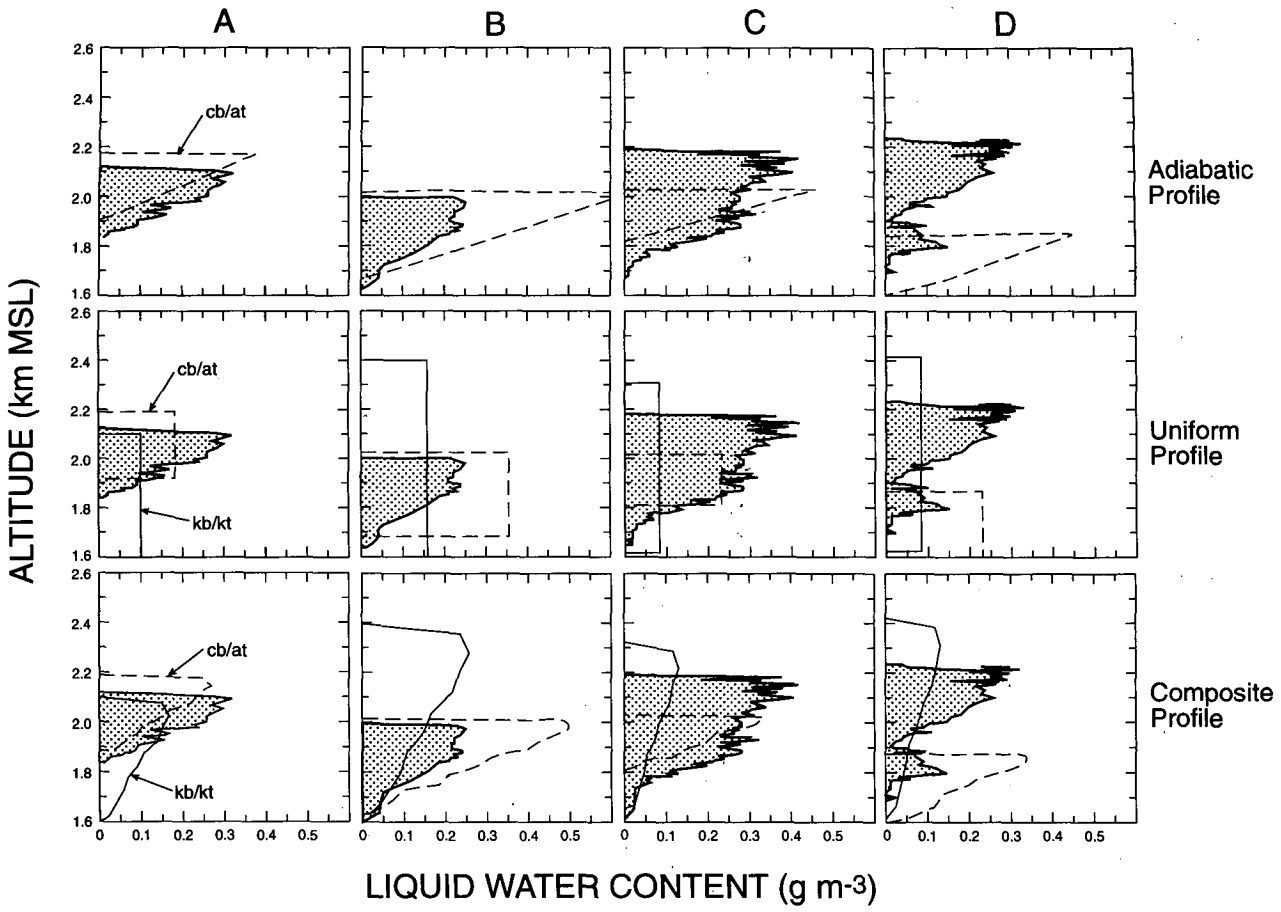

FIG. 11. Comparison of aircraft measurements of SLW (shaded area) with remote sensor estimates. Cases (columns) are listed in Table 5. The radiometer's ILW is distributed vertically according to the adiabatic, uniform, and composite methods (rows) described in the text. The solid line applies the distributions between the K_a-band radar's echo base and top (kb/kt). The dashed lines show the distributions between the ceilometer base height and the adiabatic lifted-parcel top (cb/at).

though adiabatic and composite profile shapes are similar to the actual profile shape. The radar again sensed thicker cloud than did the aircraft, which produces relatively low SLW contents throughout the cloud for the uniform and composite profiles.

Case D shows good agreement between aircraft and radiometer measurements of ILW. Remote detection of cloud base differs from the aircraft measurement by only 85 m. The ILW of the cloud is apparently substantially subadiabatic, however, and there is poor agreement between the actual cloud top and the adiabatic method cloud top. The K_a band in this case provides a better estimate of the top of the liquid cloud.

A combination of several sources of error is illustrated by these comparisons. There is some degree (see section 2) of error inherent in the liquid water measurements from the aircraft-borne instruments and the radiometer. Additional differences may be contributed by horizontal variations of liquid (section 3) since the instruments were not collocated; the aircraft sounding locations (Table 5) are 20–32 km away from the radiometer site, and the radar was 27 km away from the radiometer for two cases (Table 5). Multiple cloud layers containing liquid may also introduce error (the aircraft soundings are for the lowest layer of cloud only).

The uniform profiles are poor approximations for all four cases but may provide reasonable first guesses for a few of the profiles shown in Fig. 2. The adiabatic and composite profiles are in better agreement with the aircraft measurements in these cases and are definitely more realistic estimations of actual liquid profile shapes, in general, than the simplistic uniform profiles.

7. Summary

Variations of a combined remote sensor technique that may be useful for estimating the altitudes of supercooled liquid water in clouds have been examined. The method's basic concept is to extend the usefulness of a microwave radiometer's ILW measurement by incorporating other remote sensor observations and sim-

TABLE 5. Liquid cloud profile examples described in the text. Locations are shown in Fig. 1. Radiometer information is from the microwave radiometer and RASS data obtained at Platteville. Only radar-derived tops and bases are listed for the radar cases.

Case (date)	Facility	Time (UTC)	ILW (mm)	Base			Depth (m)	Distance from Platteville (km)
				(m)	(mb)	T (°C)		
A	Radiometer	1620	0.050	1910	790.5	−9.2	260	0
2 Mar 1991	Radar	1614	—	1600	—	—	500	27
	Aircraft	1627	0.051	1838	811.3	−9.6	207	20
B	Radiometer	1620	0.124	1680	818.4	−3.3	350	0
16 Mar 1991	Radar	1629	—	1600	—	—	800	27
	Aircraft	1611	0.055	1634	832.0	−4.0	360	32
C	Radiometer	1720	0.053	1840	805.4	−3.7	220	0
24 Feb 1993	Radar	1725	—	1620	—	—	700	0
	Aircraft	1727	0.119	1661	829.4	−4.3	526	32
D	Radiometer	2330	0.064	1600	829.1	−6.1	280	0
24 Feb 1993	Radar	2330	—	1620	—	—	800	0
	Aircraft	2350	0.063	1698	826.3	−6.8	535	30

ple models to establish the height limits and distribution of the liquid. Possible uses are for aircraft icing hazard identification, numerical model initialization, and weather modification operations. The clouds used in this study are probably well suited for the estimation of icing altitudes and liquid profiles; that is, they are totally supercooled, have little to no precipitation, and are relatively shallow. In clouds that have portions at temperatures above 0°C, some means must be available to partition the ground-sensed liquid into above- and below-freezing regimes (liquid at temperatures greater than 0°C is not an icing hazard). In precipitation, including virga, ceilometers and short-wavelength radars have problems detecting the cloud base, and radiometers may be subject to saturation of the brightness temperature in rain or heavy drizzle. In deep clouds, especially with cold tops, high concentrations of ice crystals may be formed that tend to deplete liquid. Also, the structures of these clouds tend to be quite complex with embedded layers of liquid rather than the simple single-layer model we have assumed here.

Nevertheless, these methods show some promise for estimating liquid water altitudes by remote sensing and provide a basis upon which to perform additional studies in this area. As an example, a plan for further development of an operational system, in this case for in-flight icing avoidance, could include the following elements:

- Ground-based remote sensors (ceilometer, microwave radiometer, short-wavelength radar) for real-time detection of relevant cloud parameters
- Incorporation of real-time satellite imagery and commercial airliner temperature and humidity data when and where available
- A one-dimensional cloud model tuned for the region, to provide analyses of the current situation
- A mesoscale model designed to provide a forecast (3–12 h) of three-dimensional cloud locations and liquid distribution.

The mesoscale model could be initialized on operationally available model output and run in a four-dimensional data assimilation mode using local remote sensing data (such as in Kuo et al. 1993) to adjust cloud and liquid distributions. The cloud locations and liquid profiles thus predicted could be "nudged" toward observed current conditions by comparing total integrated model liquid to the radiometer-measured ILW value, adjusting cloud base using ceilometer or radar data, and modifying cloud tops and layers using radar or satellite data. If such a real-time modeling effort is not feasible, a simpler one-dimensional cloud model could be adapted to ingest temperature sounding and remote sensing observations to analyze current cloud conditions. A final step would be to use a climatological profile, based on numerous research aircraft soundings, to estimate the vertical distribution of liquid as described in section 6.

The most difficult measurement to obtain by remote sensing for the method is the liquid cloud-top height. In addition, the cloud top as detected by satellite, rawinsonde, radar, or pilot report may not represent the top of the liquid if ice is present. The liquid may not be confined to a single layer, nor the lowest of multiple layers. Because this important parameter is difficult to measure with confidence, we have shown some alternative methods by which cloud top may be estimated from available datasets.

Acknowledgments. This research is sponsored by the National Science Foundation through an interagency agreement in response to requirements and funding by the Federal Aviation Administration's Aviation Weather Development Program. The views expressed

are those of the authors and do not necessarily represent the official policy or position of the U.S. Government. The U.S. Department of Energy Atmospheric Radiation Measurement Program provided additional support for this and related research. Ed Westwater and J. Vivekanandan contributed many useful ideas for this work. Jeff Cole, Jannelle Reynolds, and Ben Bernstein assisted with data analysis, as well as with preparation of figures. Cecelia Girz and the anonymous reviewers provided thorough reviews of the manuscript, which are greatly appreciated.

REFERENCES

Baumgardner, D. G., 1983: An analysis and comparison of five water droplet measuring instruments. *J. Climate Appl. Meteor.*, **22**, 891–910.

Bernstein, B. C., and M. K. Politovich, 1993: The production of supercooled liquid water by a secondary cold front. Preprints, *Fifth Int. Conf. on Aviation Weather Systems*, Vienna, VA, Amer. Meteor. Soc., 422–426.

Brown, B. G., T. L. Fowler, B. C. Bernstein, and G. S. Forbes, 1993: Use of pilot reports for verification of aircraft icing diagnoses and forecasts. Preprints, *Fifth Int. Conf. on Aviation Weather Systems*, Vienna, VA. Amer. Meteor. Soc., 277–281.

Bullock, C. S., J. S. Wakefield, J. M. Brundage, D. S. Walts, T. J. LeFebvre, P. A. Amstein, and L. B. Dunn, 1988: The DAR^{3}E workstation and some lessons learned from its operational use. Preprints, *Third Int. Conf. on Interactive Information and Processing Systems for Meteorology, Oceanography, and Hydrology*, Anaheim, CA., Amer. Meteor. Soc., 70–76.

Cerni, T. A., 1982: Determination of the size and concentration of cloud drops with an FSSP. *J. Climate Appl. Meteor.*, **22**, 1346–1355.

Cooper, W. A., 1988: Effects of coincidence on measurements with a forward scattering spectrometer probe. *J. Atmos. Oceanic Technol.*, **5**, 823–832.

——, W. R. Sand, M. K. Politovich, and D. L. Veal, 1984: Effects of icing on performance of a research aircraft. *J. Aircr.*, **21**, 708–715.

Gardiner, B. A., and J. Hallett, 1985: Degradation of in-cloud forward scattering spectrometer probe measurements in the presence of ice particles. *J. Atmos. Oceanic Technol.*, **2**, 171–180.

Heggli, M. F., and R. M. Rauber, 1988: The characteristics and evolution of supercooled water in wintertime storms over the Sierra Nevada: A summary of microwave radiometric measurements taken during the Sierra Cooperative Pilot Project. *J. Appl. Meteor.*, **27**, 989–1015.

Hill, G. E., 1992: Further comparisons of simultaneous airborne and radiometric measurements of supercooled liquid water. *J. Appl. Meteor.*, **31**, 397–401.

Hogg, D. C., F. O. Guiraud, J. B. Snider, M. T. Decker, and E. R. Westwater, 1983: A steerable dual-channel microwave radiometer for measurements of water vapor and liquid water in the troposphere. *J. Climate Appl. Meteor.*, **22**, 789–806.

Jacobsen, M. D., and W. M. Nunnalee, 1994: A spinning flat reflector for millimeter-wave radiometry. NOAA Tech. Mem. ERL ETL-238, 20 pp.

King, W. D., D. A. Parkin, and R. J. Handsworth, 1978: A hot-wire liquid water device having fully calculable response characteristics. *J. Appl. Meteor.*, **17**, 1809–1813.

Kuo, Y. H., Y. R. Guo, and E. R. Westwater, 1993: Assimilation of precipitable water measurements into a mesoscale numerical model. *Mon. Wea. Rev.*, **121**, 1215–1238.

Martner, B. E., and R. A. Kropfli, 1993: Observations of multi-layered clouds using K-band radar. Reprint AIAA 93-0394, 31st Aerospace Sci. Meeting, Reno, NV, 8 pp. [Available from Amer. Inst. Aeronautics and Astronautics, 370 L'Enfant Prom., SW, Washington, DC 20024.]

——, ——, L. E. Ash, and J. B. Snider, 1993a: Cloud liquid water content measurement tests using dual-wavelength radar. NOAA Tech. Memo. ERL ETL-235, 47 pp.

——, D. B. Wuertz, B. B. Stankov, R. G. Strauch, E. R. Westwater, K. S. Gage, W. L. Ecklund, C. L. Martin, and W. F. Dabberdt, 1993b: An evaluation of wind profiler, RASS, and microwave radiometer performance. *Bull. Amer. Meteor. Soc.*, **74**, 599–613.

Matrosov, S. Y., and R. A. Kropfli, 1993: Cirrus cloud studies with elliptically polarized K_a-band radar signals: A suggested approach. *J. Atmos. Oceanic Technol.*, **5**, 684–692.

May, P. T., R. G. Strauch, and K. P. Moran, 1988: The altitude coverage of temperature measurements using RASS with wind profiler radars. *Geophys. Res. Lett.*, **15**, 1381–1384.

Pobanz, B. M., J. D. Marwitz, and M. K. Politovich, 1994: Conditions associated with large-drop regions. *J. Appl. Meteor.*, **33**, 1366–1372.

Politovich, M. K., and R. Olson, 1991: An evaluation of aircraft icing forecasts for the continental United States. Preprints, *Fourth Int. Conf. on Aviation Weather Systems*, Paris, France, Amer. Meteor. Soc., 234–238.

——, B. B. Stankov, and B. E. Martner, 1992: Use of combined remote sensors for determination of aircraft icing altitudes. Preprints, *11th Int. Conf. on Cloud Physics and Precipitation*, Montreal, Quebec, Canada, Amer. Meteor. Soc., 979–982.

Popa Fotino, I. A., J. A. Schroeder, and M. T. Decker, 1986: Ground-based detection of aircraft icing conditions using microwave radiometers. *IEEE Trans. Geosci. Remote Sens.*, **GE-24**, 6, 975–982.

——, M. K. Politovich, and J. W. Hinkleman Jr., 1989: Aircraft icing conditions detected by combined remote sensors: A preliminary study. Preprints, *Third Intl. Conf. on the Aviation Weather System*, Anaheim, CA., Amer. Meteor. Soc., 173–177.

Rasmussen, R. M., B. C. Bernstein, M. Murakami, G. Stossmeister, J. Reisner, and B. Stankov, 1995: The 1990 Valentine's Day arctic outbreak. Part I: Mesoscale and microscale structure and evolution of a Colorado Front Range shallow upslope cloud. *J. Appl. Meteor.*, **34**, 1481–1511.

——, and Coauthors, 1992: Winter Icing and Storms Project (WISP). *Bull. Amer. Meteor. Soc.*, **73**, 951–974.

Rauber, R. M., D. Feng, L. O. Grant, and J. B. Snider, 1986: The characteristics and distribution of cloud water over the mountains of northern Colorado during wintertime storms. Part I: Temporal variations. *J. Climate Appl. Meteor.*, **25**, 468–488.

Rodi, A. R., and P. Spyers-Duran, 1972: Analysis of time response of airborne temperature sensors. *J. Appl. Meteor.*, **11**, 554–556.

Sassen, K., R. M. Rauber, and J. B. Snider, 1986: Multiple remote sensor observations of supercooled liquid water in a winter storm near Beaver, Utah. *J. Climate Appl. Meteor.*, **25**, 825–834.

Schubert, W. H., S. K. Cox, P. E. Ciesielski, and C. M. Johnson-Pasqua, 1987: Operation of a ceilometer during the FIRE marine stratocumulus experiment. Colorado State University, Atmospheric Science Paper No. 420.

Schultz, P., and M. K. Politovich, 1992: Toward the improvement of aircraft-icing forecasts for the continental United States. *Wea. Forecasting*, **7**, 491–500.

Snider, J. B., and D. R. Rottner, 1982: The use of microwave radiometry to determine a cloud seeding opportunity. *J. Appl. Meteor.*, **21**, 1286–1291.

Stankov, B. B., and A. Bedard, 1994: Remote sensing observations of winter aircraft icing conditions: A case study. *J. Aircr.*, **31**, 79–89.

——, B. E. Martner, and M. K. Politovich, 1995: Moisture profiling of the cloudy winter atmosphere using combined remote sensors. *J. Atmos. Oceanic Technol.*, **12**, 488–510.

——, E. R. Westwater, J. B. Snider, and R. L. Weber, 1990: Remote sensor observations during WISP90: The use of micro-

wave radiometers, RASS, and ceilometers for detection of aircraft icing conditions. NOAA Tech. Mem. ERL WPL-187, 77 pp.

——, E. R. Westwater, J. B. Snider, and R. L. Weber, 1992: Remote measurements of supercooled integrated liquid water during WISP/FAA aircraft icing program. *J. Aircr.*, **29,** 604–611.

Super, A. B., E. W. Holroyd III, B. A. Boe and J. T. McPartland, 1986: Colorado River augmentation demonstration program. Tech. Rep. 42 pp. [Available from U.S. Dept. of Interior, Bureau of Reclamation, Div. of Atmos. Resources Research, Denver, CO 80225.]

Szoke, E. J., 1989: Eye of the Denver cyclone. *Mon. Wea. Rev.*, **119,** 1283–1292.

Westwater, E. R., 1993: Ground-based microwave remote sensing of meteorological variables. *Atmospheric Remote Sensing by Microwave Radiometry,* M. A. Janssen, Ed., John Wiley & Sons, 145–213.